PHYSICAL REVIEW D **81,** 036003 (2010)

Exclusive $pp \to pp\pi^+\pi^-$ reaction: From the threshold to LHC

P. Lebiedowicz[1,*] and A. Szczurek[2,1,†]

[1]*Institute of Nuclear Physics PAN, PL-31-342 Cracow, Poland*
[2]*University of Rzeszów, PL-35-959 Rzeszów, Poland*

(Received 4 December 2009; published 9 February 2010)

We evaluate differential distributions for the four-body $pp \to pp\pi^+\pi^-$ (and $p\bar{p} \to p\bar{p}\pi^+\pi^-$) reaction which constitutes an irreducible background to three-body processes $pp \to ppM$, where M are a broad resonances in the $\pi^+\pi^-$ channel, e.g., $M = \sigma$, ρ^0, $f_0(980)$, $f_2(1275)$, $f_0(1500)$. We include both double-diffractive contribution (both Pomeron and Reggeon exchanges) as well as pion-pion rescattering contribution. The first process dominates at higher energies and small pion-pion invariant masses while the second becomes important at lower energies and higher pion-pion invariant masses. The amplitude(s) is(are) calculated in the Regge approach. We compare our results with measured cross sections for the Intersecting Storage Ring and Fermi National Accelerator Laboratory experiments. We make predictions for future experiments at the anti-Proton ANnihilation at DArmstadt (PANDA), Relativistic Heavy Ion Collider, Tevatron, and LHC energies. Differential distributions in invariant two-pion mass, pion rapidities and transverse momenta of pions are presented. The two-dimensional distribution in (y_{π^+}, y_{π^-}) is particularly interesting. The higher the incident energy, the higher preference for the same-hemisphere emission of pions. The processes considered constitute a sizeable contribution to the total nucleon-nucleon cross section as well as to pion inclusive cross section.

DOI: 10.1103/PhysRevD.81.036003 PACS numbers: 11.55.Jy, 13.75.Cs, 13.75.Lb, 13.85.Lg

I. INTRODUCTION

Diffractive processes, although very difficult from the point of view of perturbative QCD, are very attractive from the general point of view of the reaction mechanism. There are several classes of diffractive-type processes [1] in high-energy nucleon-nucleon collisions such as:

(a) elastic scattering,
(b) single-diffractive excitation of one of the nucleons,
(c) double-diffractive excitation of both participating nucleons, and
(d) central (double)-diffractive production of a simple final state.

The energy dependence of the first three types of the reaction was measured and can be nicely described [2] in a somewhat academic two-state (but fulfilling unitarity) Good-Walker model [3]. The last case was not studied in too much detail either experimentally or theoretically. At not too high energies the $\pi^+\pi^-$ and $\pi^0\pi^0$ final states give dominant contribution to double-diffractive production. The multipion and KK continuum is expected to be smaller.

There is recently a growing interest in understanding exclusive three-body reactions $pp \to ppM$ at high energies, where the meson (resonance) M is produced in the central rapidity region. Many of the resonances decay into $\pi\pi$ and/or KK channels. The representative examples are $M = \sigma, \rho^0, f_0(980), \phi, f_2(1275), f_0(1500)$, and $\chi_c(0^+)$. It is clear that these resonances are seen (or will be seen) "on" the background of a $\pi\pi$ or KK continuum.[1] Therefore a good understanding of the continuum seems indispensable. In the present analysis we concentrate on the $\pi^+\pi^-$ channel. Similar analysis can be done for $\pi^0\pi^0$ exclusive production.

At larger energies a two-Pomeron exchange mechanism dominates in central production (see [1] and references therein). In calculating the amplitude related to the double-diffractive mechanism for $pp \to pp\pi^+\pi^-$ we follow the general rules of Pumplin and Henyey [6] (for early rough estimates see also Ref. [7]). At lower energies subleading Reggeons must be included in addition to the Pomeron exchanges. We include a new mechanism relevant at lower energies (FAIR, J-PARC) relying on the exchange of two pions. We shall call this mechanism pion-pion rescattering for brevity. We discuss the interplay of all the mechanisms in a quite rich four-body phase space.

We shall present an analysis starting from the threshold and extending to the LHC energies. We think a good understanding of the reaction mechanism requires the broad range of energy. Recently in Ref. [8] an unified description in the framework of a dual model was presented for exclusive J/Ψ photoproduction, also starting from the threshold and extending to the highest available energies.

*piotr.lebiedowicz@ifj.edu.pl
†antoni.szczurek@ifj.edu.pl

[1]In general, the resonance and continuum contributions may interfere. This may produce even a dip. A good example is $f_0(980)$ production (see [4,5]).

 © 2010 The American Physical Society

II. THE πN ELASTIC CROSS SECTION

At low energies, the total cross sections for $\pi^+ p$ and $\pi^- p$ show a significant energy-dependent asymmetry defined as:

$$A_{\rm tot}^{\pi p}(W) \equiv \frac{|\sigma_{\rm tot}^{\pi^+ p}(W) - \sigma_{\rm tot}^{\pi^- p}(W)|}{\sigma_{\rm tot}^{\pi^+ p}(W) + \sigma_{\rm tot}^{\pi^- p}(W)}. \tag{2.1}$$

The total cross section tests, via the optical theorem, only the imaginary part of the scattering amplitude. In our case of the $2 \to 4$ reactions[2] we should use rather a full scattering amplitude. In contrast to the total cross section the elastic scattering cross sections for $\pi^+ p$ and $\pi^- p$ show at low energies rather small asymmetry defined as

$$A_{\rm el}^{\pi p}(W) \equiv \frac{|\sigma_{\rm el}^{\pi^+ p}(W) - \sigma_{\rm el}^{\pi^- p}(W)|}{\sigma_{\rm el}^{\pi^+ p}(W) + \sigma_{\rm el}^{\pi^- p}(W)}. \tag{2.2}$$

A reliable model should explain such details of the interaction.

Therefore to fix the parameters of our double-diffractive model we consider first elastic pion-proton scattering. The amplitude for the elastic scattering of pions on nucleons is written in the simplified Regge-like form:

$$\begin{aligned}\mathcal{M}_{\pi^\pm p\to\pi^\pm p}(s,t) = {} & {\rm i}sC_{\mathbb{P}}\left(\frac{s}{s_0}\right)^{\alpha_{\mathbb{P}}(t)-1}\exp\left(\frac{B_{\pi N}^{\mathbb{P}}}{2}t\right) \\ & + (a_f + {\rm i})sC_f\left(\frac{s}{s_0}\right)^{\alpha_{\mathbb{R}}(t)-1}\exp\left(\frac{B_{\pi N}^{\mathbb{R}}}{2}t\right) \\ & \pm (a_\rho - {\rm i})sC_\rho\left(\frac{s}{s_0}\right)^{\alpha_{\mathbb{R}}(t)-1}\exp\left(\frac{B_{\pi N}^{\mathbb{R}}}{2}t\right).\end{aligned} \tag{2.3}$$

The first term describes exchange of the leading (Pomeron) trajectory while the next terms describe the subleading isoscalar (f_2) and isovector (ρ) Reggeon exchanges. The parameters $a_f = -0.860895$ and $a_\rho = -1.16158$ in order to assure the proper phase of the amplitude as dictated by corresponding signature factor. The strength parameters $C_{\mathbb{P}}$, C_f, C_ρ are taken from the Donnachie-Landshoff model [9] for total cross section:

$$\begin{gathered}C_{\mathbb{P}} = 13.63\ {\rm mb}, \qquad C_f = 31.79\ {\rm mb}, \\ C_\rho = 4.23\ {\rm mb}.\end{gathered} \tag{2.4}$$

This means that our effective phenomenological model describes the available total cross sections. The Pomeron and Reggeon trajectories determined from elastic and total cross sections are given in the form ($\alpha_i(t) = \alpha_i(0) + \alpha_i' t$):

$$\alpha_{\mathbb{P}}(t) = 1.0808 + 0.25t, \qquad \alpha_{\mathbb{R}}(t) = 0.5475 + 0.93t. \tag{2.5}$$

The values of the intercept $\alpha_{\mathbb{P}}(0)$ and $\alpha_{\mathbb{R}}(0)$ are also taken from the Donnachie-Landshoff model [9] for consistency. The slope parameter can be written as

$$B_{\pi N}(W_{\pi N}) = B_0 + 2\alpha_i' \ln\left(\frac{s}{s_0}\right). \tag{2.6}$$

We take $\alpha_i' = 0.25/0.93$ for Pomeron and Reggeon exchanges, respectively. The slope parameter $B_{\pi N}$, taken the same for the Pomeron and Reggeons, must be fitted to the data. From the fit to the data [10] we find $B_0 = 5.5\ {\rm GeV}^{-2}$. The effective slope observed in t-distributions is much larger ($B_{\rm eff} = 7$–$10\ {\rm GeV}^{-2}$ for $P_{\rm lab} = 3$–200 GeV [10]).

The differential elastic cross section is expressed with the help of the scattering amplitude as

$$\frac{d\sigma_{\rm el}}{dt} = \frac{1}{16\pi s^2}|\mathcal{M}(s,t)|^2. \tag{2.7}$$

The differential distributions $d\sigma_{\rm el}/dt$ for both $\pi^+ p$ and $\pi^- p$ elastic scattering for three incident-beam momenta of $P_{\rm lab} = 5$ GeV, $P_{\rm lab} = 50$ GeV, and $P_{\rm lab} = 200$ GeV are shown in Fig. 1. Under a detailed inspection one can observe that the local slope parameter

$$B_{\rm eff}(t) \equiv \frac{d}{dt}\ln\left(\frac{d\sigma_{\rm el}}{dt}\right) \tag{2.8}$$

is t-dependent and is slightly larger for $\pi^- p$ than for $\pi^+ p$. Such an effect was observed experimentally in Ref. [10]. The local slope decreases with increasing $|t|$. A rather good description of experimental $d\sigma_{\rm el}/dt$ is achieved.

Our one-parameter ($B_{\pi N}$) model here is consistent with the simple Donnachie-Landshoff model for the total cross section [9]. A more refined model should include absorption effects due to pion-nucleon rescatterings. The analysis of absorption effects clearly goes beyond the scope of the present paper. Our model sufficiently well describes the πN data and includes absorption effects in an effective way.[3] This has advantage for the $pp \to pp\pi\pi$ reaction discussed in the present paper where the πN absorption effects do not need to be included explicitly. This considerably simplifies the calculation for the $2 \to 4$ reaction and actually this makes the calculation of the $2 \to 4$ reaction feasible.

Before we go to the $pp \to pp\pi^+\pi^-$ reaction, we have to discuss the parameters of the πN interaction. The strength parameters of the Pomeron and Reggeon couplings are taken from the Donnachie-Landshoff analysis of the total cross section in several hadronic reactions [9] as discussed above. The only free parameters—the slope parameters—are adjusted to the elastic $\pi^+ p$ and $\pi^- p$ scattering. With $B_{\mathbb{P}} = 5.5\ {\rm GeV}^{-2}$ and $B_{\mathbb{R}} = 4\ {\rm GeV}^{-2}$ we nicely describe the existing experimental data for πp scattering as can be seen from Fig. 2 (solid lines). The

[2] $2 \to 4$ reaction denotes a type of the reaction with two initial and four final particles.

[3] The deviation at large $|t|$, seen in Fig. 1 can be "cured" using nonlinear Regge trajectories as shown e.g. in Ref. [11] (see also references therein). For simplicity we use simple linear trajectories, but further improvements are possible.

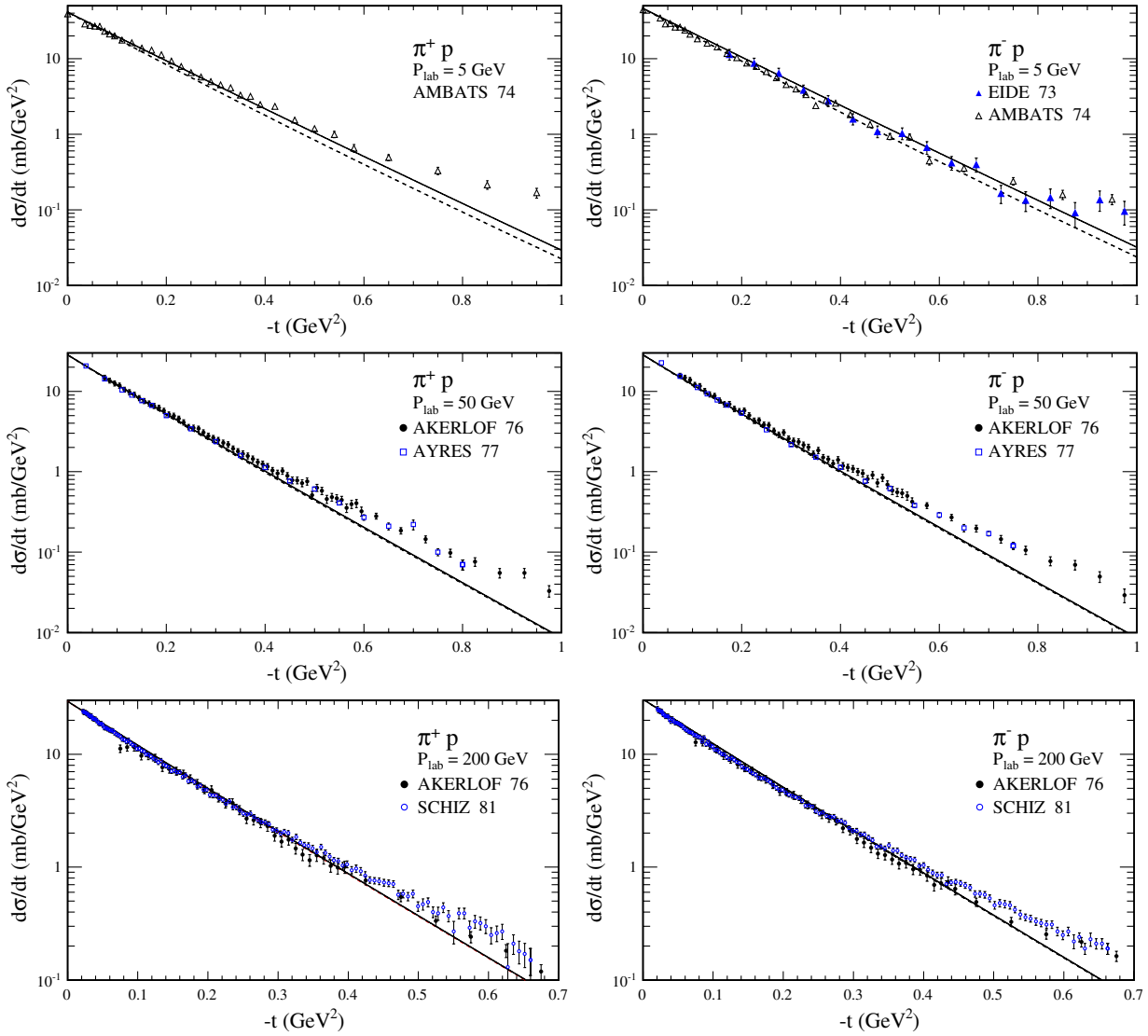

FIG. 1 (color online). Differential distributions for $\pi^+ p$ (left) and $\pi^- p$ (right) elastic scattering for different energies calculated with the amplitude (2.3) and parameters as given in the text. In this calculation the slope parameter was taken as $B_{\pi N} = 5.5\ \mathrm{GeV}^{-2}$ (dashed line). A fit to the world πN elastic scattering data suggests that the value of the Reggeon slope may be slightly smaller than the value of the Pomeron slope. The solid line shows such a result. The details are explained when discussing Fig. 2. The experimental data are taken from Ref. [10].

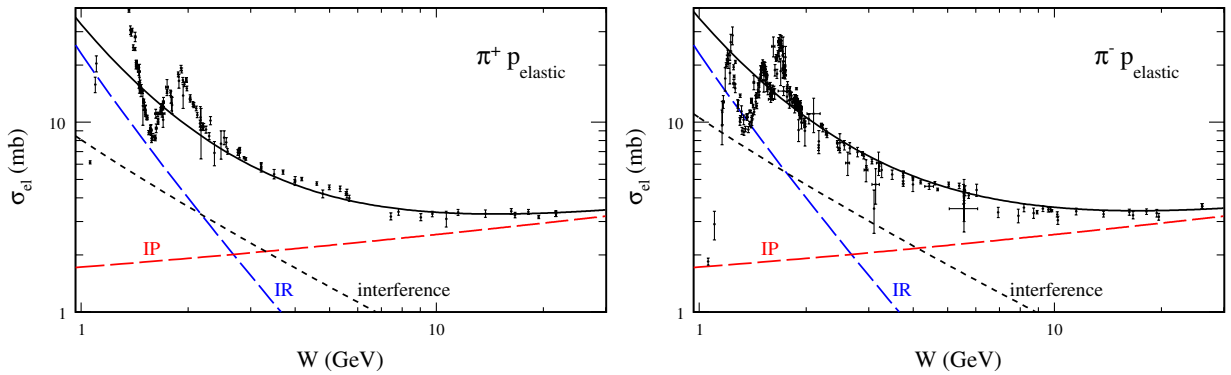

FIG. 2 (color online). The integrated cross section for πN elastic scattering as a function of center-of-mass energy. The experimental data are taken from Ref. [27].

long-dashed lines show Pomeron ($\mathbb{P}$) and Reggeon ($\mathbb{R}$) contributions and the short-dashed lines their interference term. In the Regge approach, the cross section at high energies is dominated by Pomeron exchange. The Reggeon exchange dominates in the resonance region. There is also a region of energies where the interference term dominates. This is different than for the total cross section, which is just a sum of the Pomeron and Reggeon terms. We get a nice description of the data for $\sqrt{s} > 2.5$ GeV. The region below contains resonances and is therefore very difficult for modeling.

Having fixed the parameters we can proceed to our four-body $pp \to pp\pi^+\pi^-$ reaction.

III. CENTRAL DOUBLE-DIFFRACTIVE CONTRIBUTION

The general situation is sketched in Fig. 3. The corresponding amplitude for the $pp \to pp\pi^+\pi^-$ ($p\bar{p} \to p\bar{p}\pi^+\pi^-$) process (with four-momenta $p_a + p_b \to p_1 + p_2 + p_3 + p_4$) can be written as

$$\begin{aligned}\mathcal{M}^{pp\to pp\pi\pi} = {} & M_{13}(t_1, s_{13})F(t_a)\frac{1}{t_a - m_\pi^2}F(t_a)M_{24}(t_2, s_{24}) \\ & + M_{14}(t_1, s_{14})F(t_b)\frac{1}{t_b - m_\pi^2} \\ & \times F(t_b)M_{23}(t_2, s_{23}),\end{aligned} \tag{3.1}$$

where M_{ik} denotes ''interaction'' between nucleon $i = 1$ (forward nucleon) or $i = 2$ (backward nucleon) and one of the two pions $k = 3$ (π^+), $k = 4$ (π^-). In the Regge phenomenology they can be written as

$$\begin{aligned}M_{ik}(t_i, s_{ik}) = {} & \mathrm{i}s_{ik}C_{\mathbb{P}}\left(\frac{s_{ik}}{s_0}\right)^{\alpha_{\mathbb{P}}(t_i)-1}\exp\left(\frac{B_{\mathbb{P}}}{2}t_i\right) \\ & + (a_f + \mathrm{i})s_{ik}C_f\left(\frac{s_{ik}}{s_0}\right)^{\alpha_{\mathbb{R}}(t_i)-1}\exp\left(\frac{B_{\mathbb{R}}}{2}t_i\right) \\ & \pm (a_\rho - \mathrm{i})s_{ik}C_\rho\left(\frac{s_{ik}}{s_0}\right)^{\alpha_{\mathbb{R}}(t_i)-1}\exp\left(\frac{B_{\mathbb{R}}}{2}t_i\right).\end{aligned} \tag{3.2}$$

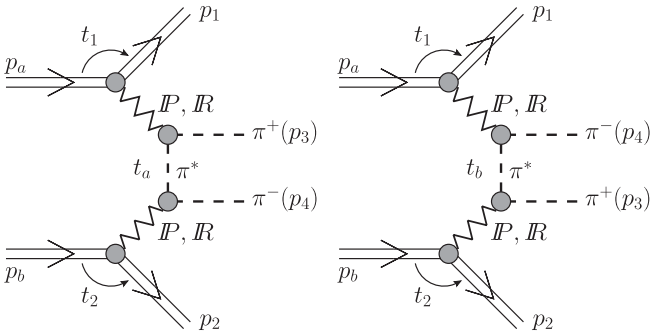

FIG. 3. A sketch of the dominant mechanisms of exclusive production of $\pi^+\pi^-$ pairs at high energies.

Above $s_{ik} = W_{ik}^2$, where W_{ik} is the center-of-mass energy in the (i, k) subsystems. The third term is with the sign plus if $k = 3$ and with the sign minus if $k = 4$. The normalization constants $(C_{\mathbb{P}}, C_f, C_\rho)$ can be estimated from the fit to the total πN cross section (2.4). The values of the Regge trajectories (2.5) are also taken from the Donnachie-Landshoff model [9]. At high πN subsystem energies $W_{ik} > 20$ GeV only the Pomeron exchange survive.

The extra form factors $F(t_a)$ and $F(t_b)$ ''correct'' for off-shellness of the intermediate pions in the middle of the diagrams shown in Fig. 3. In the following they are parametrized as

$$F(t_{a,b}) = \exp\left(\frac{t_{a,b} - m_\pi^2}{\Lambda_{\mathrm{off},E}^2}\right), \tag{3.3}$$

i.e., normalized to unity on the pion-mass-shell. In the following for brevity we shall use notation $t_{a,b}$ which means t_a or t_b. In general, the parameter $\Lambda_{\mathrm{off},E}$ is not known but in principle could be fitted to the (normalized) experimental data. From our general experience in hadronic physics we expect $\Lambda_{\mathrm{off},E} \sim 1$ GeV. How to extract $\Lambda_{\mathrm{off},E}$ will be discussed in the Results section.

The parametrization [9] can be used only for $W_{ik} >$ 2–3 GeV. Below $W_{ik} = 2$ GeV resonances in πN subsystems are present. In principle, their contribution could and should be included explicitly.[4,5] The amplitude (3.1) with (3.2) is used to calculate the corresponding cross section including limitations of the four-body phase-space. To exclude regions of resonances we shall ''correct'' the parametrization (3.1) with (3.2) by multiplying by a purely phenomenological smooth cut-off correction factor:

$$f_{\mathrm{cont}}^{\pi N}(W_{ik}) = \frac{\exp(\frac{W_{ik}-W_0}{a})}{1 + \exp(\frac{W_{ik}-W_0}{a})}. \tag{3.4}$$

The parameter W_0 gives the position of the cut and parameter a describes how sharp the cutoff is. The first parameter can have a significant influence on the results. We shall take $W_0 = 2$–3 GeV and $a = 0.1$–0.5 GeV. For large energies $f_{\mathrm{cont}}^{\pi N}(W_{ik}) \approx 1$ and close to kinematical threshold $W_{ik} = m_\pi + M_N$: $f_{\mathrm{cont}}^{\pi N}(W_{ik}) \approx 0$. In our calculation, if not otherwise mentioned, we use $W_0 = 2$ GeV and $a = 0.2$ GeV.

IV. PION-PION RESCATTERING

For the $pp \to pp\pi^+\pi^-$ or $p\bar{p} \to p\bar{p}\pi^+\pi^-$ reactions there is another type of semidiffractive contribution shown in Fig. 4.

[4]The higher the center-of-mass energy the smaller the relative resonance contribution.

[5]In the standard terminology the resonances belong to single-diffractive contribution to be distinguished from double-diffractive contribution discussed here.

Similarly as for the $p\bar{p} \to N\bar{N}f_0(1500)$ reaction (see [12]) the amplitude squared—averaged over the initial and summed over the final polarization states—for these processes can be written as:

$$\overline{|\mathcal{M}|^2} = \frac{1}{4}\Bigg[(E_a+m)(E_1+m)\Bigg(\frac{\mathbf{p}_a^2}{(E_a+m)^2}+\frac{\mathbf{p}_1^2}{(E_1+m)^2}-\frac{2\mathbf{p}_a\cdot\mathbf{p}_1}{(E_a+m)(E_1+m)}\Bigg)\Bigg] \times 2\frac{g_{\pi NN}^2}{(t_1-m_\pi^2)^2}F_{\pi NN}^2(t_1)\times|\mathcal{M}_{\pi^{0*}\pi^{0*}\to\pi^+\pi^-}(s_{34},\hat{t},\hat{u};t_1,t_2)|^2\times\frac{g_{\pi NN}^2}{(t_2-m_\pi^2)^2}F_{\pi NN}^2(t_2) \times\Bigg[(E_b+m)(E_2+m)\Bigg(\frac{\mathbf{p}_b^2}{(E_b+m)^2}+\frac{\mathbf{p}_2^2}{(E_2+m)^2}-\frac{2\mathbf{p}_b\cdot\mathbf{p}_2}{(E_b+m)(E_2+m)}\Bigg)\Bigg]\times 2. \tag{4.1}$$

In the formula above m is the mass of the nucleon, E_a, E_b and E_1, E_2 are energies of initial and outgoing nucleons, $\mathbf{p}_a$, $\mathbf{p}_b$ and $\mathbf{p}_1$, $\mathbf{p}_2$ are corresponding three-momenta, and m_π is the pion mass. The factor $g_{\pi NN}$ is the pion-nucleon coupling constant and is relatively well known [13] ($\frac{g_{\pi NN}^2}{4\pi}=13.5$–$14.6$). In our calculations the coupling constants are taken as $g_{\pi NN}^2/4\pi = 13.5$.

At high-energies the pion-pion scattering amplitude of the subprocess $\pi^{0*}\pi^{0*} \to \pi^+\pi^-$ with virtual initial pions can be written, similarly as for πN scattering (here only ρ-Reggeon exchange is relevant):

$$\begin{aligned}&\mathcal{M}_{\pi^{0*}\pi^{0*}\to\pi^+\pi^-}(s_{34},\hat{t},\hat{u};t_1,t_2)\\ &=(a_\rho-\mathrm{i})s_{34}C_\rho^{\pi\pi}\Big(\frac{s_{34}}{s_0}\Big)^{\alpha_{\mathbb{R}}(\hat{t})-1}\exp\Big(\frac{B_{\pi\pi}}{2}\hat{t}\Big)F_{\pi^{0*}}(t_1)F_{\pi^{0*}}(t_2)\\ &\quad+(a_\rho-\mathrm{i})s_{34}C_\rho^{\pi\pi}\Big(\frac{s_{34}}{s_0}\Big)^{\alpha_{\mathbb{R}}(\hat{u})-1}\exp\Big(\frac{B_{\pi\pi}}{2}\hat{u}\Big)\\ &\quad\times F_{\pi^{0*}}(t_1)F_{\pi^{0*}}(t_2).\end{aligned} \tag{4.2}$$

Above $C_\rho^{\pi\pi} = 16.38$ mb is obtained assuming Regge factorization [14]. We have parametrized the $\hat{t}$, $\hat{u}$ dependences in the exponential form. The slope parameter is not well known; however, it may be expected to be $B_{\pi\pi} \sim$ 4–6 GeV^{-2}. In our calculation, if not otherwise mentioned, we use $B_{\pi\pi} = 4$ GeV^{-2}. In the formula above $F_{\pi^*}(t_{1,2})$ are extra correction factors due to off-shellness of initial pions. We use exponential form factors of the type (3.3). To exclude regions of resonances we correct the Regge parametrization (4.2) by multiplying by a factor $f_{\mathrm{cont}}^{\pi N}(W_{34})$ (as in (3.4)).

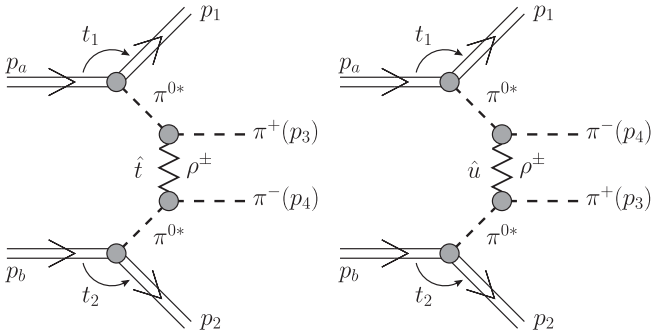

FIG. 4. A sketch of the high-energy pion-pion rescattering mechanisms.

In the case of central production of pion pairs not far from the threshold rather large transferred four-momenta squared t_1 and t_2 are involved and one has to include the non-point-like and off-shellness nature of the particles involved in corresponding vertices. This is incorporated via $F_{\pi NN}(t_1)$ or $F_{\pi NN}(t_2)$ vertex form factors. In the meson exchange approach [15] they are parametrized in the monopole form as

$$F_{\pi NN}(t_{1,2}) = \frac{\Lambda^2-m_\pi^2}{\Lambda^2-t_{1,2}}. \tag{4.3}$$

Typical values of the form factor parameters are $\Lambda =$ 1.2–1.4 GeV [15]; however, the Gottfried Sum Rule violation prefers smaller $\Lambda \approx 0.8$ GeV [16].

V. THE DIFFERENTIAL CROSS SECTION

The differential cross section for the $2 \to 4$ reaction is given as

$$d\sigma = \frac{1}{2s}\overline{|\mathcal{M}|^2}(2\pi)^4\delta^4(p_a+p_b-p_1-p_2-p_3-p_4) \times\frac{d^3p_1}{(2\pi)^3 2E_1}\frac{d^3p_2}{(2\pi)^3 2E_2}\frac{d^3p_3}{(2\pi)^3 2E_3}\frac{d^3p_4}{(2\pi)^3 2E_4}. \tag{5.1}$$

This can be written in a useful form:

$$d\sigma = \frac{1}{2s}\overline{|\mathcal{M}|^2}\delta^4(p_a+p_b-p_1-p_2-p_3-p_4)\frac{1}{(2\pi)^8}\frac{1}{2^4} \times(dy_1p_{1t}dp_{1t}d\phi_1)(dy_2p_{2t}dp_{2t}d\phi_2)(dy_3d^2p_{3t}) \times(dy_4d^2p_{4t}). \tag{5.2}$$

This can be further simplified:

$$d\sigma = \frac{1}{2s}\overline{|\mathcal{M}|^2}\delta(E_a+E_b-E_1-E_2-E_3-E_4) \times\delta^3(p_{1z}+p_{2z}+p_{3z}+p_{4z})\frac{1}{(2\pi)^8}\frac{1}{2^4} \times(dy_1p_{1t}dp_{1t}d\phi_1)(dy_2p_{2t}dp_{2t}d\phi_2)dy_3dy_4d^2p_m. \tag{5.3}$$

Above we have introduced an auxiliary quantity:

$$\mathbf{p}_m = \mathbf{p}_{3t} - \mathbf{p}_{4t}. \tag{5.4}$$

We choose transverse momenta of the outgoing nucleons (p_{1t}, p_{2t}), azimuthal angles of outgoing nucleons (ϕ_1, ϕ_2) and rapidity of the pions (y_3, y_4) as independent kinematically complete variables. Then the cross section can be calculated as:

$$\begin{aligned} d\sigma = & \sum_k \mathcal{J}^{-1}(p_{1t}, \phi_1, p_{2t}, \phi_2, y_3, y_4, p_m, \phi_m)|_k \\ & \times \frac{\overline{|\mathcal{M}(p_{1t}, \phi_1, p_{2t}, \phi_2, y_3, y_4, p_m, \phi_m)|^2}}{2\sqrt{s(s-4m^2)}} \frac{1}{(2\pi)^8} \frac{1}{2^4} \\ & \times p_{1t} dp_{1t} d\phi_1 p_{2t} dp_{2t} d\phi_2 \frac{1}{4} dy_3 dy_4 d^2 p_m, \end{aligned} \tag{5.5}$$

where the δ functions have been totally eliminated and k denotes symbolically discrete solutions of the set of equations for energy and momentum conservation:

$$\begin{aligned} \sqrt{s} - E_3 - E_4 &= \sqrt{m_{1t}^2 + p_{1z}^2} + \sqrt{m_{2t}^2 + p_{2z}^2}, \\ -p_{3z} - p_{4z} &= p_{1z} + p_{2z}, \end{aligned} \tag{5.6}$$

where m_{1t} and m_{2t} are transverse masses of outgoing nucleons. The solutions of Eq. (5.6) depend on the values of integration variables: $p_{1z} = p_{1z}(p_{1t}, p_{2t}, p_{3t}, p_{4t}, \phi_1, \phi_2, y_3, y_4)$ and $p_{2z} = p_{2z}(p_{1t}, p_{2t}, p_{3t}, p_{4t}, \phi_1, \phi_2, y_3, y_4)$.

In Eq. (5.5) an extra Jacobian of the transformation $(y_1, y_2) \to (p_{1z}, p_{2z})$ has appeared:

$$\mathcal{J}_k = \left| \frac{p_{1z}(k)}{\sqrt{m_{1t}^2 + p_{1z}(k)^2}} - \frac{p_{2z}(k)}{\sqrt{m_{2t}^2 + p_{2z}(k)^2}} \right|. \tag{5.7}$$

In the limit of high energies and central production, i.e., $p_{1z} \gg 0$ (very forward nucleon1), $-p_{2z} \gg 0$ (very backward nucleon2) the Jacobian becomes a constant $\mathcal{J} \to \frac{1}{2}$.

To calculate the total cross section one has to calculate the 8-dimensional integral (see Eq. (5.5)) numerically. This requires some care.

In the next section we shall show our predictions for several differential distributions in different variables.

VI. RESULTS

Before we go to our four-body reaction let us focus for a moment on $\pi^0\pi^0 \to \pi^+\pi^-$ on-shell scattering. In Fig. 5 we show the total (angle-integrated) cross section for the $\pi^0\pi^0 \to \pi^+\pi^-$ process. We include both the pion-pion rescattering contribution obtained from partial wave analysis [4] as well as contribution from the Regge phenomenology at higher energies. The parameters of the Regge amplitude for the $\pi\pi \to \pi\pi$ scattering were obtained in Ref. [14] from different isospin combinations of nucleon-(anti)nucleon and pion-nucleon scattering assuming Regge factorization. For our case of $\pi^0\pi^0 \to \pi^+\pi^-$ reaction only the ρ-Reggeon exchange is relevant. We show predictions

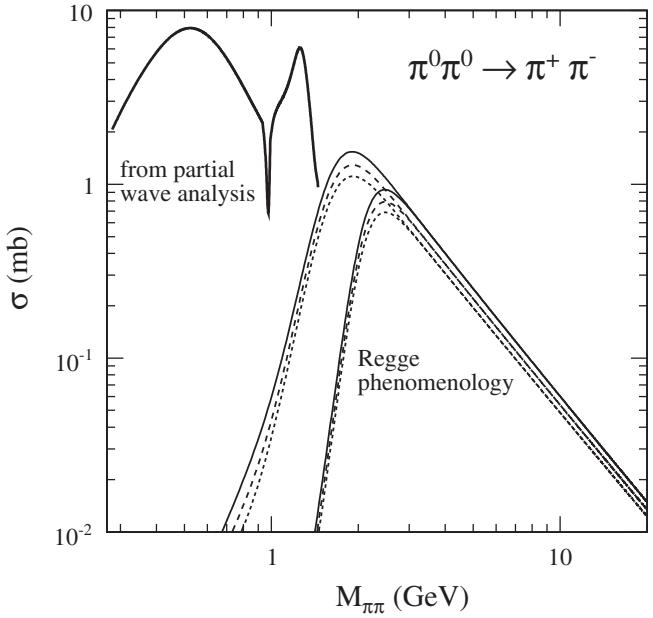

FIG. 5. The angle-integrated cross section for the reaction $\pi^0\pi^0 \to \pi^+\pi^-$. We present contributions obtained from partial wave analysis [4] and Regge phenomenology [14] for corrected ($W_0 = 1.5$, 2 GeV and $a = 0.2$ GeV in Eq. (3.4)) extrapolations to low energies.

for the Regge contribution for corrected ($W_0 = 1.5$, 2 GeV and $a = 0.2$ GeV in Eq. (3.4)) extrapolations to low energies and for different values of the slope parameter $B_{\pi\pi} = 4$ GeV^{-2} (dotted lines), $B_{\pi\pi} = 5$ GeV^{-2} (dashed lines) and $B_{\pi\pi} = 6$ GeV^{-2} (solid lines). A relatively good matching is achieved without extra fitting the model pa-

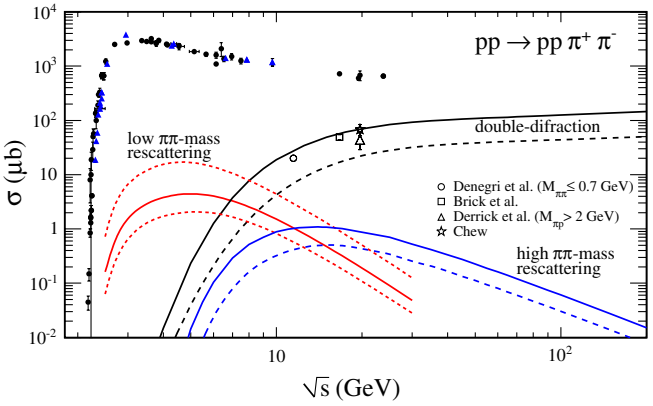

FIG. 6 (color online). Cross section for the $pp \to pp\pi^+\pi^-$ reaction integrated over phase space as a function of the center-of-mass energy. We compare the pion-pion rescattering and double-diffractive contributions with the experimental data (open symbols represent DPE contribution from Refs. [17–20] and filled symbols show the cross sections for the $pp \to pp\pi^+\pi^-$ reaction (black circles) from Ref. [21] and the $p\bar{p} \to p\bar{p}\pi^+\pi^-$ reaction (blue triangles) from Ref. [22]). The theoretical uncertainties for these contributions are shown in addition.

TABLE I. Full-phase-space integrated cross section (in μb) for exclusive double-diffractive $\pi^+\pi^-$ production at selected center-of-mass energies and different values of the off-shell-form factor parameters. Here $W_0 = 2$ GeV and $a = 0.2$ GeV in Eq. (3.4). No absorption effects were included explicitly.

$F(t_{a,b})$	$\Lambda^2_{\rm off}$ (GeV^2)	$W = 5.5$ GeV	$W = 200$ GeV	$W = 1960$ GeV	$W = 14$ TeV
$\exp((t_{a,b} - m_\pi^2)/\Lambda^2_{{\rm off},E})$	0.5	0.1	50.3	96.4	179.1
	1	0.6	146.2	287.2	535.2
$(\Lambda^2_{{\rm off},M} - m_\pi^2)/(\Lambda^2_{{\rm off},M} - t_{a,b})$	0.5	0.02	18.9	35.6	66
	1	0.18	64.6	125.2	232.8
$((\Lambda^2_{{\rm off},D} - m_\pi^2)/(\Lambda^2_{{\rm off},D} - t_{a,b}))^2$	0.5	0.31	83.6	164.2	306.5
	1	1.15	217.5	437.9	822.4

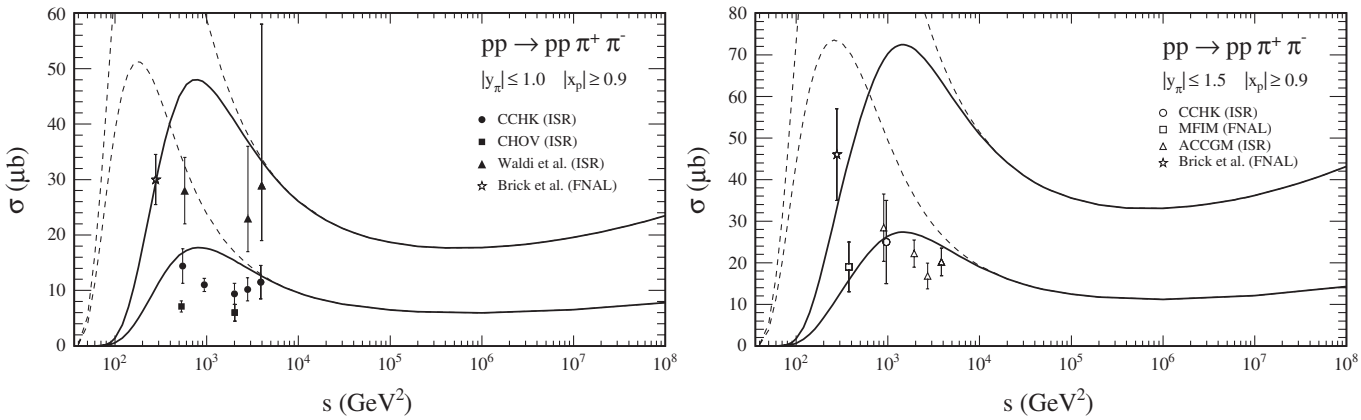

FIG. 7. Cross section for the $pp \to pp\pi^+\pi^-$ reaction integrated over phase space with cuts relevant for a given experiments [18,28–30]. The experimental value from [30] (open circle) was obtained for the different cut $\Delta y = |y_p - y_\pi| > 2$. We show results for different values of the parameter $\Lambda^2_{{\rm off},E} = 0.5$ GeV^2 (lower lines), $\Lambda^2_{{\rm off},E} = 1$ GeV^2 (upper lines) and for the naive (dashed lines) and corrected (solid lines with $W_0 = 2$ GeV and $a = 0.2$ GeV) extrapolations to low energies.

rameters. In the following we shall focus on the higher-$M_{\pi\pi}$ Regge component which dominates at higher energies (see Fig. 6).

In Fig. 6 we present the total cross section for the $pp \to pp\pi^+\pi^-$ reaction, i.e., the cross section integrated over full phase space, as a function of the center-of-mass energy. We show theoretical predictions from the models calculations with $\Lambda = 0.8$ GeV and $\Lambda^2_{{\rm off},E} = 1$ GeV^2 (solid lines) and $\Lambda^2_{{\rm off},E} = 0.5$ GeV^2 (dashed lines). The bottom dotted line was obtained with $\Lambda = 0.8$ GeV and $\Lambda^2_{{\rm off},E} = 0.5$ GeV^2 while the top dotted line with $\Lambda = 1.4$ GeV and $\Lambda^2_{{\rm off},E} = 2$ GeV^2. Details of the low-$M_{\pi\pi}$ rescattering contribution can be found in Ref. [4]. The search for a double Pomeron exchange mechanism contribution leads to an upper limits of $\simeq 20$ μb (for $M_{\pi\pi} \leq 0.7$ GeV) [17], (49 ± 5.5) μb [18], (44 ± 15) μb [19] and (68 ± 16) μb [20]. The experimental value of the cross section taken from [19] was obtained for $M_{p\pi} > 2$ GeV and no limitation on $M_{\pi\pi}$, it reduces however to 9 μb for $M_{\pi\pi} \leq 0.6$ GeV [19]. For comparison we show the full cross sections for the $pp \to pp\pi^+\pi^-$ reaction (filled black circles) from Ref. [21] and for the $p\bar{p} \to p\bar{p}\pi^+\pi^-$ reaction (filled blue triangles) from Ref. [22] which are more than 1 mb for $(2.5 < \sqrt{s} < 10)$ GeV.[6] Clearly for low energies ($\sqrt{s} < 20$ GeV) neither exclusive double diffraction nor pion-pion rescattering constitute the dominant mechanism. Here the production of single and double resonances is the dominant mechanism (see, e.g., [4]). The mechanism of the resonant production is rather complicated and will not be discussed in the present analysis.

The results depend on the value of the nonperturbative, *a priori* unknown parameter of the form factor responsible for off-shell effects. In Table I we have collected integrated cross sections for selected energies and different values of model parameters. We show how the uncertainties of the form factor parameters affect our final results.

In Fig. 7 we show predictions of the double-diffractive component for different values of the parameter $\Lambda^2_{{\rm off},E} = 0.5$ GeV^2 (lower lines), $\Lambda^2_{{\rm off},E} = 1$ GeV^2 (upper lines) and for naive (dashed lines) and corrected (solid lines with $W_0 = 2$ GeV and $a = 0.2$ GeV) extrapolations to low energies. The experimental cuts on the rapidity of both pions and on longitudinal momentum fractions of both outgoing protons are included when comparing our results with

[6]This is a significant contribution to the total pp cross section.

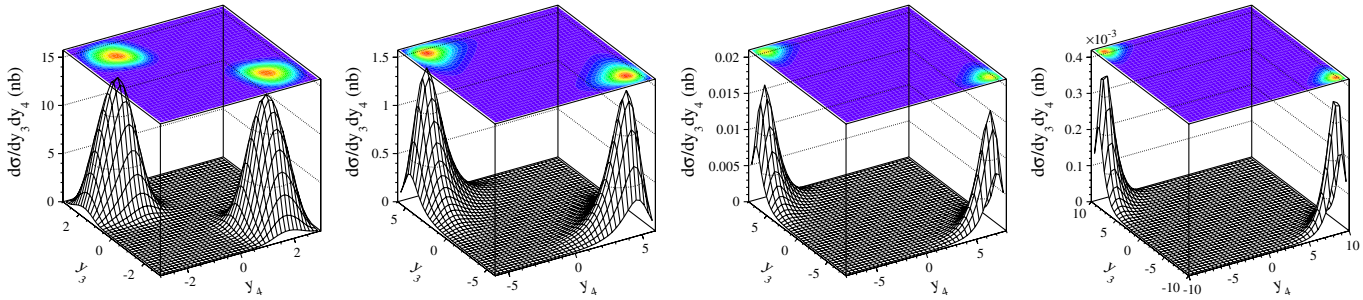

FIG. 8 (color online). Differential cross section in (y_3, y_4) for the high-$M_{\pi\pi}$ pion-pion rescattering contribution for different incident energies: $W = 5.5$ (PANDA), 200 (RHIC), 1960 (Tevatron), 14000 (LHC) GeV.

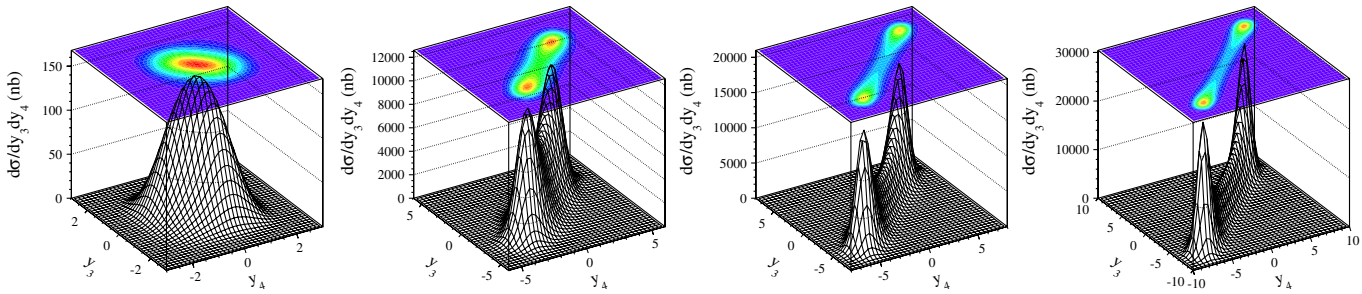

FIG. 9 (color online). Differential cross section in (y_3, y_4) for the double-diffractive contribution for different incident energies: $W = 5.5$ (PANDA), 200 (RHIC), 1960 (Tevatron), 14000 (LHC) GeV.

existing experimental data. Although not all the data are in good agreement with the predictions, their general trend follows the theoretical expectations. No absorption effects were included in this calculation. In general, the higher the energy the higher the absorption effects. The bare (without absorption effects) cross section rises with energy. The absorption corrections are expected to lower or even stop the rise. Consistent inclusion of absorption effects is rather difficult and will not be studied here.

The distribution in the (y_3, y_4) space is particularly interesting. In Figs. 8 and 9 we show distributions for the pion-pion rescattering and double-diffractive contributions, respectively. In this calculation the cutoff parameter $\Lambda^2_{\mathrm{off},E} = 1$ GeV^2. The cross section for the pion-pion rescattering drops quickly with the center-of-mass energy. The rescattered pions are emitted preferentially in different hemispheres, π^+ at positive y_3 and π^- at negative y_4 or π^+ at negative y_3 and π^- at positive y_4. The bare cross section for the double-diffractive contribution grows with energy. At high energies the pions are emitted preferentially in the same hemispheres, i.e., $y_3, y_4 > 0$ or $y_3, y_4 < 0$. While at low energies (anti-Proton ANnihilation at DArmstadt [PANDA]) both contributions (exclusive double diffraction and pion-pion rescattering) overlap, at high energies (Relativistic Heavy Ion Collider [RHIC], Tevatron, LHC) they are well separated, i.e., can, at least in principle, be measured.

At high energies the diffractive contribution seems more interesting. The camel-like shape of the y_3, y_4 distribution requires a separate discussion. In our calculation we in-

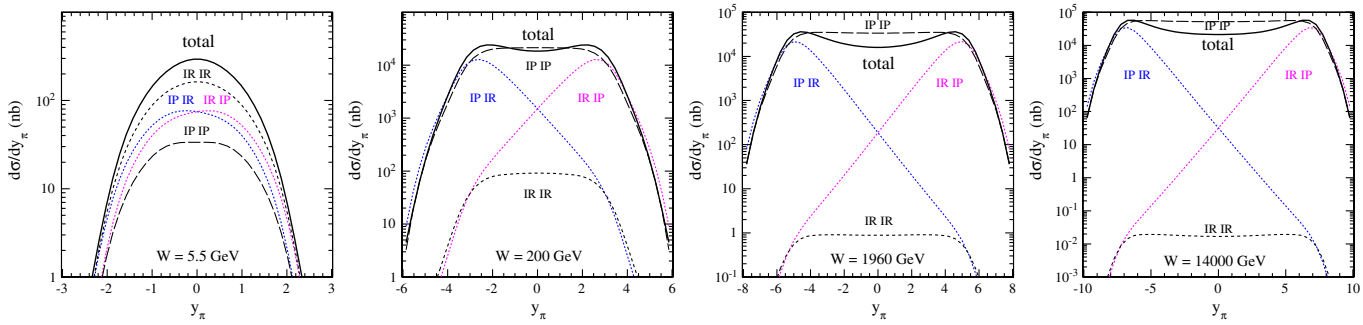

FIG. 10 (color online). Rapidity distribution of pions (π^+ or π^-) for different center-of-mass energies. The different lines correspond to the situation when only some components in the amplitude are included. The details are explained in the main text.

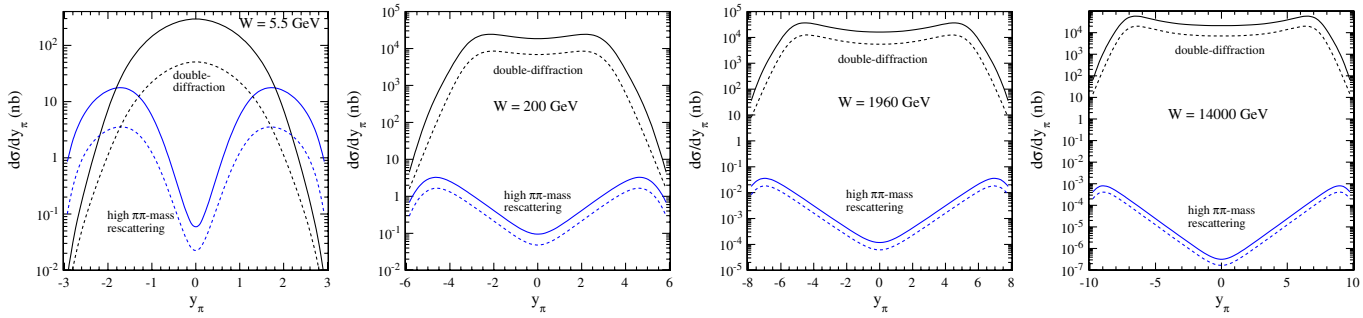

FIG. 11 (color online). Differential cross section $d\sigma/dy_\pi$ for the double-diffractive and high-$M_{\pi\pi}$ pion-pion rescattering contributions at the PANDA, RHIC, Tevatron and LHC energies. The solid lines was obtained with $\Lambda^2_{\text{off},E} = 1$ GeV^2 and dashed lines with $\Lambda^2_{\text{off},E} = 0.5$ GeV^2.

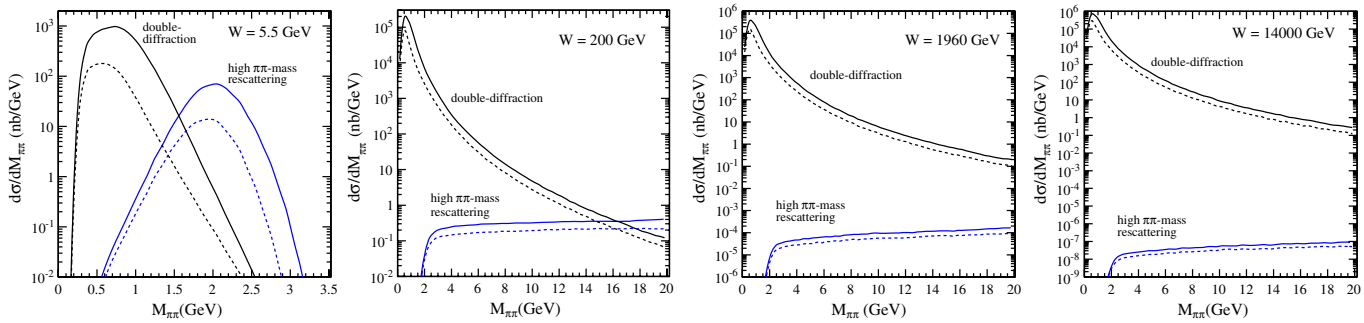

FIG. 12 (color online). Differential cross section $d\sigma/dM_{\pi\pi}$ for diffractive and high-$M_{\pi\pi}$ pion-pion rescattering contributions at the PANDA, RHIC, Tevatron, and LHC energies. The solid lines was obtained with $\Lambda^2_{\text{off},E} = 1$ GeV^2 and dashed lines with $\Lambda^2_{\text{off},E} = 0.5$ GeV^2.

clude both Pomeron and Reggeon exchanges. In Fig. 10 we show the cross section in $y_\pi = y_3 = y_4$ for all ingredients included (thick solid line) and when only Pomeron exchanges are included (long-dashed line), separately for Pomeron-Reggeon and Reggeon-Pomeron exchanges (dotted lines) and when only Reggeon exchanges are included (dashed line). In this calculation the cutoff parameter $\Lambda^2_{\text{off},E} = 1$ GeV^2. At low energies all individual cross sections when isolated are comparable. They strongly interfere leading to an increase of the cross section. At higher energies each of the ''isolated'' cross sections peak in different regions of y_3 or y_4. The $\mathbb{P} \otimes \mathbb{P}$ cross section peaks at midrapidities of pions, while $\mathbb{P} \otimes \mathbb{R}$ and $\mathbb{R} \otimes \mathbb{P}$ at backward and forward pion rapidities, respectively. When interfering the three components in the amplitude produce significant (camel-like) enhancements of the cross section at forward/backward rapidities. It would be desirable to identify the camel-like structure experimentally.[7] At even more forward/backward rapidities one may expect single-diffraction contributions (e.g., diffractive production of nucleon resonances and their decays) not included in the present analysis. This will be discussed elsewhere [23].

In Fig. 11 we compare distributions of pion rapidities y_π for exclusive double diffraction and high-$M_{\pi\pi}$ pion-pion rescattering at the PANDA, RHIC, Tevatron and LHC energies.

In Fig. 12 we show the two-pion invariant-mass distribution at the PANDA, RHIC, Tevatron, and LHC energies. At the lowest energy the pion-pion rescattering and the double-diffractive components strongly overlap. While the double-diffractive component dominates at low two-pion invariant masses, the pion-pion rescattering component dominates at large invariant masses. This dependence can be used to improve purity of one of the two components by imposing extra cuts. At the Tevatron and LHC energies the double-diffractive component dominates over the pion-pion rescattering in the whole range of $M_{\pi\pi}$.

Finally we show distributions in transverse momentum of the pions (Fig. 13). The double-diffractive component dominates over the pion-pion rescattering component. The pions are produced preferentially back-to-back. The smearing in $p_{t\pi}$ around zero as well as with respect to $\phi_{\pi\pi} = \pi$ (relative azimuthal angle between charged pions) is caused by the disbalance of transverse momenta of exchanged Pomerons and/or Reggeons from both pro-

[7]The ALICE experiment seems to be able to study the dependence because of relatively low threshold on pion transverse momenta.

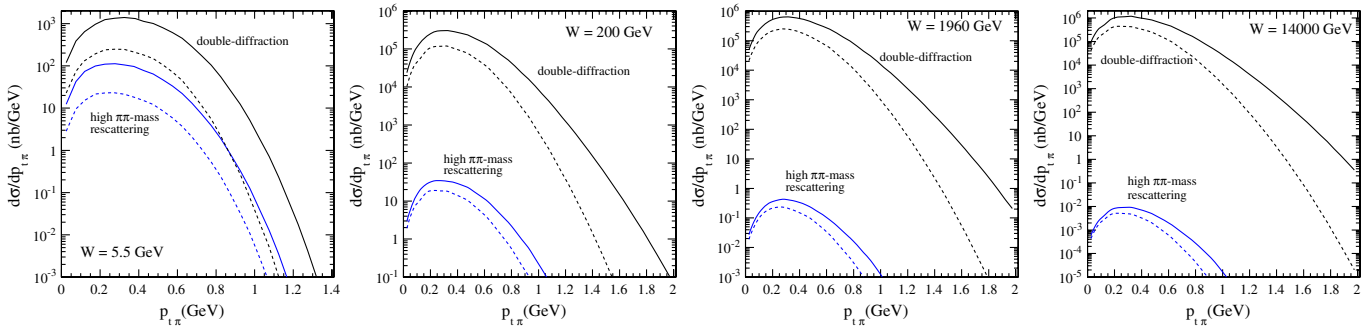

FIG. 13 (color online). Differential cross section $d\sigma/dp_{t\pi}$ for diffractive and pion-pion rescattering contributions at the PANDA, RHIC, Tevatron, and LHC energies. The solid lines was obtained with $\Lambda^2_{\mathrm{off},E} = 1$ GeV^2 and the dashed lines with $\Lambda^2_{\mathrm{off},E} = 0.5$ GeV^2.

ton/antiproton lines. Whether the distributions can be measured at the LHC requires Monte Carlo studies of the ALICE detector.

VII. OUTLOOK

A. Beyond the Born approximation

In the present, intentionally simplified, analysis we have performed calculation in the Born approximation with the form factor parameter roughly adjusted to existing "low-energy" experimental data. In a more microscopic approach one has to include higher-order diagrams shown in Figs. 14 and 15.

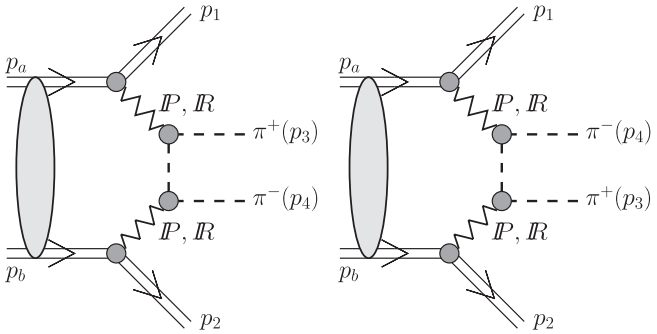

FIG. 14. Diagrams representing the absorption effects due to proton-proton interaction.

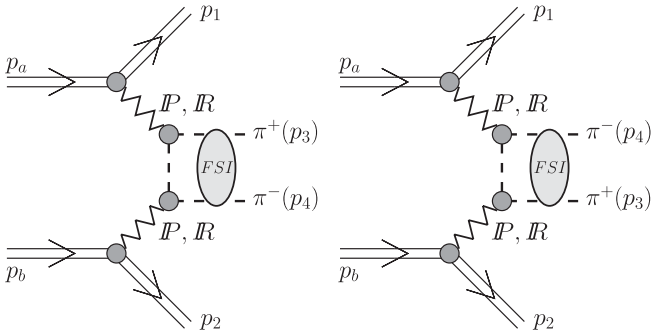

FIG. 15. Diagrams representing pion-pion final state interaction.

The first type of the interaction was studied, e.g., for three-body reactions [24]. For the four-body reaction discussed here a similar effect is expected, i.e., a large energy-dependent damping of the cross section which is often embodied in the soft gap survival probability.

When going from the Born (Fig. 3) to the diagrams with the pion-pion FSI (Fig. 15) the following replacement is formally required:

$$\frac{F^A_{\mathrm{off}}(k)F^B_{\mathrm{off}}(k)}{k^2-m_\pi^2} \to \int \frac{d^4k}{(2\pi)^4}\,\frac{1}{k^2-m_\pi^2}\,\frac{F^A_{\mathrm{off}}(k,k_3)}{k_3^2-m_\pi^2}\,\frac{F^B_{\mathrm{off}}(k,k_4)}{k_4^2-m_\pi^2} \times \sum_{ij}\mathcal{M}^{\text{off-shell}}_{\pi_i\pi_j\to\pi^\pm\pi^\mp}(k_3k_4\to p_3p_4), \quad (7.1)$$

where the sum runs over different isospin combinations of pions. In general the integral above is complicated (singularities, unknown elements), the vertex form factors (A and B) with two-pions being off-mass-shell are not well known, and even the off-shell matrix element is not fully under control. Usually serious simplifications are done to make the calculation useful on a practical level. Limiting to the S-wave ($L = 0$) one can correct the Born amplitude by a phenomenological function which causes an enhancement close to the two-pion threshold and damping at $M_{\pi\pi} \sim 0.8$ GeV. Dealing with higher partial waves is more complicated. At even larger $M_{\pi\pi}$ the interaction becomes absorptive and was not much studied. Some work can be found in Ref. [14]. Obviously much more theoretical effort is required.

The second type of diagrams leads approximately to a redistribution of the strength but seems to modify the pion-pion integrated cross section very little [6]. The effect of pion-pion FSI must be, however, included if the spectrum of invariant mass is studied. At high invariant masses one may expect also a strong damping due to absorption in the pion-pion subsystem. Only low-invariant-mass spectra were studied in the past experiments [25]. The experiments at LHC could study the potential damping of large-mass dipion production and therefore could shed more light on the not fully understood problem of absorption effects in a few-body hadronic systems, so important in understanding,

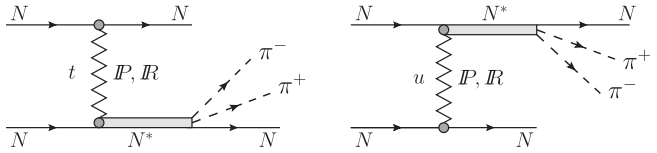

FIG. 16. Resonance contributions to the $pp \to pp\pi^+\pi^-$ reaction through diffractive single resonance excitation (DSRE).

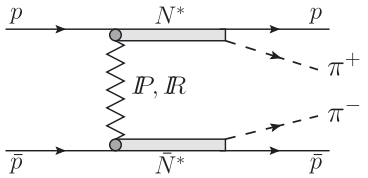

FIG. 17. Resonance contributions to the $p\bar{p} \to p\bar{p}\pi^+\pi^-$ reaction through diffractive double resonance excitation (DDRE).

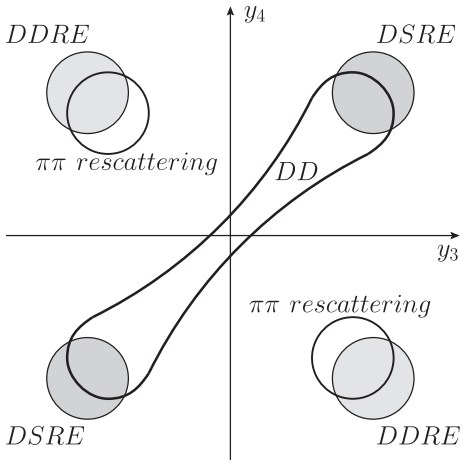

FIG. 18. A schematic localization in the (y_3, y_4) space of different mechanisms for the $pp \to pp\pi^+\pi^-$ or $p\bar{p} \to p\bar{p}\pi^+\pi^-$ reactions at high energies. The acronyms used in the figure are explained in the main text.

e.g., the exclusive production of the Higgs boson discussed recently in the literature.

B. Other not included processes at high energies

Up to now we have discussed only central double-diffractive (CDD) contribution to the $pp \to pp\pi^+\pi^-$ reaction. In general, there are also contributions with diffractive single or double proton/antiproton excitations followed by the resonance decays shown in Figs. 16 and 17. The first mechanism contributes both to the $pp \to pp\pi^+\pi^-$ and $p\bar{p} \to p\bar{p}\pi^+\pi^-$ reaction while the second mechanism only to the $p\bar{p} \to p\bar{p}\pi^+\pi^-$ reaction at high energy.[8]

Can these processes be separated from the CDD contribution? The general situation at high energy is sketched in Fig. 18. The CDD contributions discussed in this paper lay along the diagonal $y_3 = y_4$ and the classical DPE in the center $y_3 \approx y_4$. The diffractive single resonance excitation (DSRE) contribution[9] is expected at y_3, $y_4 \sim y_{\text{beam}}$ or y_3, $y_4 \sim y_{\text{target}}$, i.e., situated at the end points of the CDD contribution. The diffractive double resonance excitation (DDRE) contribution is expected at ($y_3 \sim y_{\text{beam}}$ and $y_4 \sim y_{\text{target}}$) or ($y_3 \sim y_{\text{target}}$ and $y_4 \sim y_{\text{beam}}$), i.e., well separated from the CDD contribution discussed in the present paper. The Tevatron is the only place where one could look at the DDRE contribution, never studied so far at high energies, when it is clearly separated from other mechanisms (CDD, DSRE).

VIII. CONCLUSIONS

We have estimated cross sections and calculated several differential observables for the exclusive $pp \to pp\pi^+\pi^-$ and $p\bar{p} \to p\bar{p}\pi^+\pi^-$ reactions. Both double-diffractive and pion-pion rescattering processes were considered. The full amplitude was parametrized in terms of subsystem amplitudes. Only continuum processes (classical DPE) were included in the present analysis.

In the first case the energy dependence of the amplitudes of πN subsystems was parametrized in the Regge form which describes total and elastic cross section for πN scattering. This parametrization includes both leading pomeron trajectory as well as subleading reggeon exchanges. Even at relatively high-energies the inclusion of reggeon exchanges is crucial as amplitudes with different combination of exchanges interfere or/and πN subsystem energies can be relatively small $W_{\pi N} < 10$ GeV. The latter happens when y_{π^+}, $y_{\pi^-} \gg 0$ or y_{π^+}, $y_{\pi^-} \ll 0$. In this region of the phase space one can expect a competition of the single diffractive mechanism. In the literature mainly the total single diffractive was calculated. We leave the estimation of the SD mechanism contributions to the $pp\pi^+\pi^-$ channel for a separate study.

The integrated cross section of the central double-diffractive component grows slowly with incident energy if absorption effects are ignored. In principle, the absorption effects may even reverse the trend.

In the second case the amplitude for the pion-pion subprocess was parametrized using a recent phase shift analysis at the low pion-pion energies and a Regge form of the continuum obtained by assumption of Regge factorization. The factorization assumption is made to estimate the process contribution.

At high energy the two contributions occupy different parts of the phase space, have different energy dependence, and in principle can be resolved experimentally. The interference of amplitudes of the both processes is almost negligible.

[8]At low energy the double Δ isobar excitation contributes to $pp \to pp\pi^+\pi^-$.

[9]The Roper resonance excitation is a good example.

The energy dependence of the ''diffractive'' central production of two-pions is quite different than the one for elastic scattering, single-, or double-diffraction. This is due to the specificity of the reaction, where rather the subsystem energies dictate the energy dependence of the process.

At high energies we find a preference for the same hemisphere (same-sign rapidity) emission of π^+ and π^-. At Intersecting Storage Ring energies the same size emission is about 50% while at LHC energies the same hemisphere emission constitutes about 90% of all cases.

In the present paper we have concentrated on central exclusive production of two pions. In the analysis we have excluded several resonance contributions. Formally they belong to the category (b) or (c) and not (d) which we consider in the present analysis. But the distinction between the different categories is a bit arbitrary and may be quite involved experimentally. Some early LHC experiments will concentrate on single-diffractive production of resonances [26]. Some of those processes could contribute to the final channel discussed here. This problem is quite unexplored and requires a future analysis. We plan future work on this subject.

ACKNOWLEDGMENTS

We are indebted to Mike Albrow and Valeri Khoze for an exchange of information and Wolfgang Schäfer for a discussion. This study was partially supported by the Polish grant of MNiSW No. N202 249235.

[1] G. Alberi and G. Goggi, Phys. Rep. **74**, 1 (1981).
[2] A. B. Kaidalov, Phys. Rep. **50**, 157 (1979).
[3] M. L. Good and W. D. Walker, Phys. Rev. **120**, 1857 (1960).
[4] P. Lebiedowicz, A. Szczurek, and R. Kamiński, Phys. Lett. B **680**, 459 (2009).
[5] D. M. Alde *et al.* (GAMS Collaboration), Phys. Lett. B **397**, 350 (1997).
[6] J. Pumplin and F. S. Henyey, Nucl. Phys. **B117**, 377 (1976).
[7] Ya. I. Azimov, E. M. Levin, V. A. Khoze, and M. G. Ryskin, Sov. J. Nucl. Phys. **21**, 215 (1975).
[8] R. Fiore, L. L. Jenkovszky, V. K. Magas, S. Melis, and A. Prokudin, Phys. Rev. D **80**, 116001 (2009)
[9] A. Donnachie and P. V. Landshoff, Phys. Lett. B **296**, 227 (1992).
[10] A. Eide *et al.*, Nucl. Phys. **B60**, 173 (1973); I. Ambats *et al.*, Phys. Rev. D **9**, 1179 (1974); C. W. Akerlof *et al.*, Phys. Rev. D **14**, 2864 (1976); D. S. Ayres *et al.*, Phys. Rev. D **15**, 3105 (1977); A. Schiz *et al.*, Phys. Rev. D **24**, 26 (1981).
[11] R. Fiore, L. L. Jenkovszky, V. Magas, F. Paccanoni, and A. Papa, Eur. Phys. J. A **10**, 217 (2001).
[12] A. Szczurek and P. Lebiedowicz, Nucl. Phys. **A826**, 101 (2009).
[13] T. E. O. Ericson, B. Loiseau, and A. W. Thomas, Phys. Rev. C **66**, 014005 (2002).
[14] A. Szczurek, N. N. Nikolaev, and J. Speth, Phys. Rev. C **66**, 055206 (2002).
[15] R. Machleidt, K. Holinde, and Ch. Elster, Phys. Rep. **149**, 1 (1987); D. V. Bugg and R. Machleidt, Phys. Rev. C **52**, 1203 (1995).
[16] A. Szczurek and J. Speth, Nucl. Phys. **A555**, 249 (1993); B. C. Pearce, J. Speth, and A. Szczurek, Phys. Rep. **242**, 193 (1994); J. Speth and A. W. Thomas, Adv. Nucl. Phys. **24**, 83 (1997).
[17] D. Denegri *et al.* (France-Soviet-Union Collaboration), Nucl. Phys. **B98**, 189 (1975).
[18] D. H. Brick *et al.*, Z. Phys. C **19**, 1 (1983).
[19] M. Derrick *et al.*, Phys. Rev. Lett. **32**, 80 (1974).
[20] D. M. Chew, Nucl. Phys. **B82**, 422 (1974).
[21] E. Pickup *et al.*, Phys. Rev. **125**, 2091 (1962); E. L. Hart *et al.*, Phys. Rev. **126**, 747 (1962); A. M Eisner *et al.*, Phys. Rev. **138**, B670 (1965); E. Gellert *et al.*, Phys. Rev. Lett. **17**, 884 (1966); G. Alexander *et al.*, Phys. Rev. **154**, 1284 (1967); A. P. Colleraine and U. Nauenberg, Phys. Rev. **161**, 1387 (1967); W. Chinowsky *et al.*, Phys. Rev. **171**, 1421 (1968); S. P. Almeida *et al.*, Phys. Rev. **174**, 1638 (1968); R. Ehrlich *et al.*, Phys. Rev. Lett. **21**, 1839 (1968); G. Kayas *et al.*, Nucl. Phys. **B5**, 169 (1968); C. Caso *et al.*, Nuovo Cimento A **55**, 66 (1968); **33**, 671 (1976); C. D. Brunt *et al.*, Phys. Rev. **187**, 1856 (1969); G. Yekutieli *et al.*, Nucl. Phys. **B18**, 301 (1970); E. Colton *et al.*, Phys. Rev. D **3**, 1063 (1971); J. G. Rushbrooke *et al.*, Phys. Rev. D **4**, 3273 (1971); H. Boggild *et al.*, Nucl. Phys. **B27**, 285 (1971); J. Le Guyader *et al.*, Nucl. Phys. **B35**, 573 (1971); D. R. F. Cochran *et al.*, Phys. Rev. D **6**, 3085 (1972); W. Burdett *et al.*, Nucl. Phys. **B48**, 13 (1972); B. Y. Oh *et al.* (MFIM Collaboration), FERMILAB Report No. FERMILAB-PUB-77-114-E 1977; M. Derrick *et al.*, Phys. Rev. D **9**, 1215 (1974); Zh. S. Takibaev *et al.*, Yad. Fiz. **21**, 1015 (1975); F. H. Cverna *et al.*, Phys. Rev. C **23**, 1698 (1981); S. A. Azimov *et al.*, Yad. Fiz. **34**, 77 (1981); F. Shimizu *et al.*, Nucl. Phys. **A386**, 571 (1982); L. G. Dakhno *et al.*, Sov. J. Nucl. Phys. **37**, 540 (1983); D. H. Brick *et al.*, Z. Phys. C **19**, 1 (1983); J. Johanson *et al.* (PROMICE/WASA Collaboration), Nucl. Phys. **A712**, 75 (2002); S. Abd El-Bary *et al.* (COSY-TOF Collaboration), Eur. Phys. J. A **37**, 267 (2008).
[22] H. C. Dehne *et al.*, Phys. Rev. **136**, B843 (1964); C. Walck *et al.*, Nucl. Phys. **B100**, 61 (1975); M. A. Jabiol *et al.*, Nucl. Phys. **B127**, 365 (1977); C. K. Chen *et al.*, Phys. Rev. D **17**, 42 (1978); D. R. Ward *et al.*, Nucl. Phys. **B172**, 302 (1980); D. E. Zissa *et al.*, Phys. Rev. D **22**, 2642 (1980); M. Yu. Bogolyubsky *et al.*, Yad. Fiz. **43**, 350 (1986); B. V. Batyunya *et al.*, Yad. Fiz. **46**, 1117 (1987); [Sov. J. Nucl. Phys. **46**, 650 (1987)]; L. Bertolotto *et al.* (JETSET Collaboration), Phys. Lett. B **345**, 325 (1995);

A. Buzzo *et al.* (JETSET Collaboration), Z. Phys. C **76**, 475 (1997).

[23] P. Lebiedowicz and A. Szczurek, to be presented in the future.

[24] W. Schäfer and A. Szczurek, Phys. Rev. D **76**, 094014 (2007).

[25] T. Akesson *et al.*, Nucl. Phys. **B264**, 154 (1986).

[26] R. Orava, ''Diffractive and Electromagnetic Processes at the LHC,'' Trento, 2010.

[27] C. Amsler *et al.* (Particle Data Group), Phys. Lett. B **667**, 1 (2008), http://pdg.lbl.gov/2009/hadronic-xsections/.

[28] R. Waldi, K. R. Schubert, and K. Winter, Z. Phys. C **18**, 301 (1983).

[29] L. Baksay *et al.* (ACCGM Collaboration), Phys. Lett. B **61**, 89 (1976); H. De Kerret *et al.* (CHOV Collaboration), Phys. Lett. B **68**, 385 (1977); D. Drijard *et al.*, (CCHK Collaboration), Nucl. Phys. **B143**, 61 (1978); B. Y. Oh *et al.* (MFIM Collaboration), FERMILAB Report No. FERMILAB-PUB-77-114-E 1977.

[30] M. Della Negra *et al.* (CCHK Collaboration), Phys. Lett. B **65**, 394 (1976).